LASER INTERFEROMETER GRAVITATIONAL WAVE OBSERVATORY

LIGO Laboratory / LIGO Scientific Collaboration

LIGO-E0900268-v3 *ADVANCED LIGO* 01/11/10

Engineering Specifications of an adaptive ring heater in the input optics of Advanced LIGO

Muzammil A. Arain, Luke F. Williams, and David H. Reitze

Distribution of this document:
LIGO Science Collaboration

This is an internal working note
of the LIGO Project.

California Institute of Technology
LIGO Project – MS 18-34
1200 E. California Blvd.
Pasadena, CA 91125
Phone (626) 395-2129
Fax (626) 304-9834
E-mail: info@ligo.caltech.edu

Massachusetts Institute of Technology
MIT NW22-295
185 Albany Street
Cambridge, MA 02139 USA
Phone (617) 253-4824
Fax (617) 253-7014
E-mail: info@ligo.mit.edu

LIGO Hanford Observatory
P.O. Box 1970
Mail Stop S9-02
Richland WA 99352
Phone 509-372-8106
Fax 509-372-8137

LIGO Livingston Observatory
P.O. Box 940
Livingston, LA 70754
Phone 225-686-3100
Fax 225-686-7189

http://www.ligo.caltech.edu/

Table of Contents

1 Introduction

1.1 Purpose and Scope

This document describes the engineering specifications for the Adaptive Optical Element (AOE) to be used in the IO section of Advanced LIGO. The AOE is intended to provide a 'control knob' to adjust the mode matching between the IMC and RC. This AOE is a part of PMMT design. Depending upon the performance of other IO components, we may or may not need to use this in a control loop.

1.2 LIGO Documents

1. Muzammil A. Arain, Luke F. Williams, and David H. Reitze, "Pre Mode Matching Telescope Parameters, Adaptive Mode matching and Diagnostics," LIGO technical note, LIGO- T0900407 available at: https://dcc.ligo.org/cgi-bin/private/DocDB/ShowDocument?docid=6003.
2. Muzammil A. Arain et al., "Adaptive control of modal properties of optical beams using photothermal effects," Manuscript in preparation, LIGO DCC document LIGO-P0900116.
3. Luke F. Williams, Drwaing for Adaptive Optical Element, LIGO Drawing LIGO-D0901578.
4. Muzammil A. Arain and David H. Reitze, "In Vacuum Alignment and Calibration Procedure for Adaptive Optical Element," LIGO Inspection report, LIGO-E0900328.
5. Straight Interferometer IOT Layout, LIGO-D0902284, available at https://dcc.ligo.org/cgi-bin/private/DocDB/ShowDocument?docid=5943.
6. Folded Interferometer IOT Layout, LIGO-D0902285, available at https://dcc.ligo.org/cgi-bin/private/DocDB/ShowDocument?docid=5944.

1.3 Acronyms

ROC: Radius of Curvature

PRC: Power Recycling Cavity

SRC: Signal Recycling Cavity

RC: Recycling Cavity

IMC: Input Mode Cleaner

PMMT: Pre-mode Matching Telescope

IOT: Input Output Optics Table

FOM: Figure of Merit

2 Optical layout of the PMMT

The modes of the input mode cleaner (IMC) and recycling cavities (PRC) are different, requiring a mode matching telescope between IMC and the PRC. The details of the optical layout are presented in Ref. 1. The optical layout is shown in Fig. 1 here for reference.

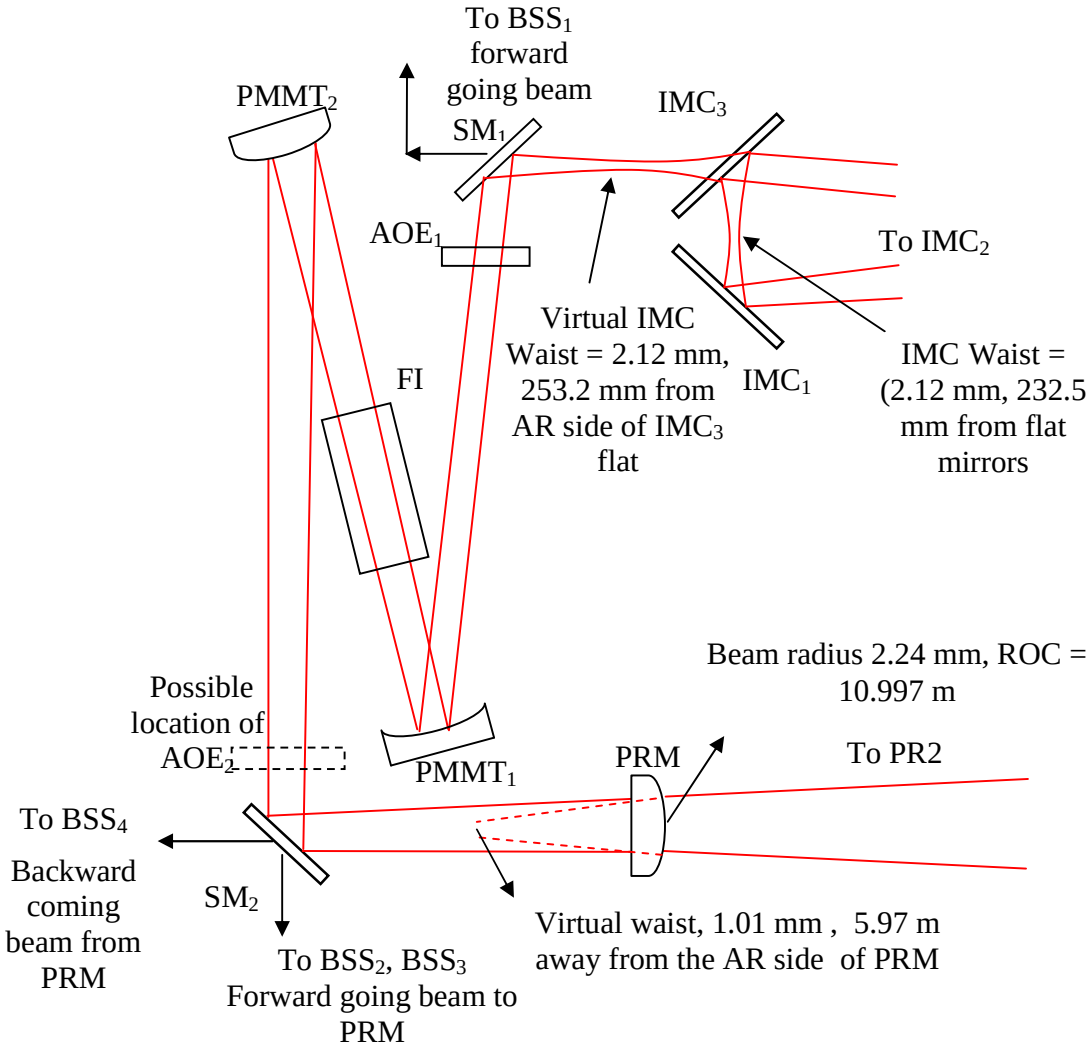

Fig. 1: Optical Layout of HAM2 Table including details of pre ode matching telescope for the H1 and L1 interferometers. The numbers shown are for straight interferometers. AOE stands for Adaptive Optical Element. Folded interferometer numbers are mentioned in Table 1.

3 Description of AOE

The concept of an AOE is shown in Fig. 2 and explained in detail in reference [2]. Here an optic is heated via four independent heaters in thermal contact with the optic arranged along t the periphery. These heaters induces photothermal effects in the optic and due to dn/dT and thermal expansion α, produce a parabolic temperature gradient in the radial direction. This creates a lens in the material. By controlling the amount of heating (electrical input to the heaters), the lens focal power can be controlled. The details of the proposed system are described in Ref. 1.

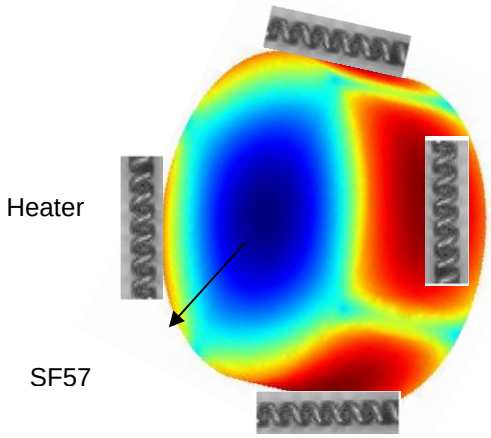

Fig. 2: conceptual layout of the AOE

3.1 Advanced LIGO AOE

The Advanced LIGO version of AOE is shown in Fig. 3. The detail drawings and dimensions are presented in Ref. 1 and 3.

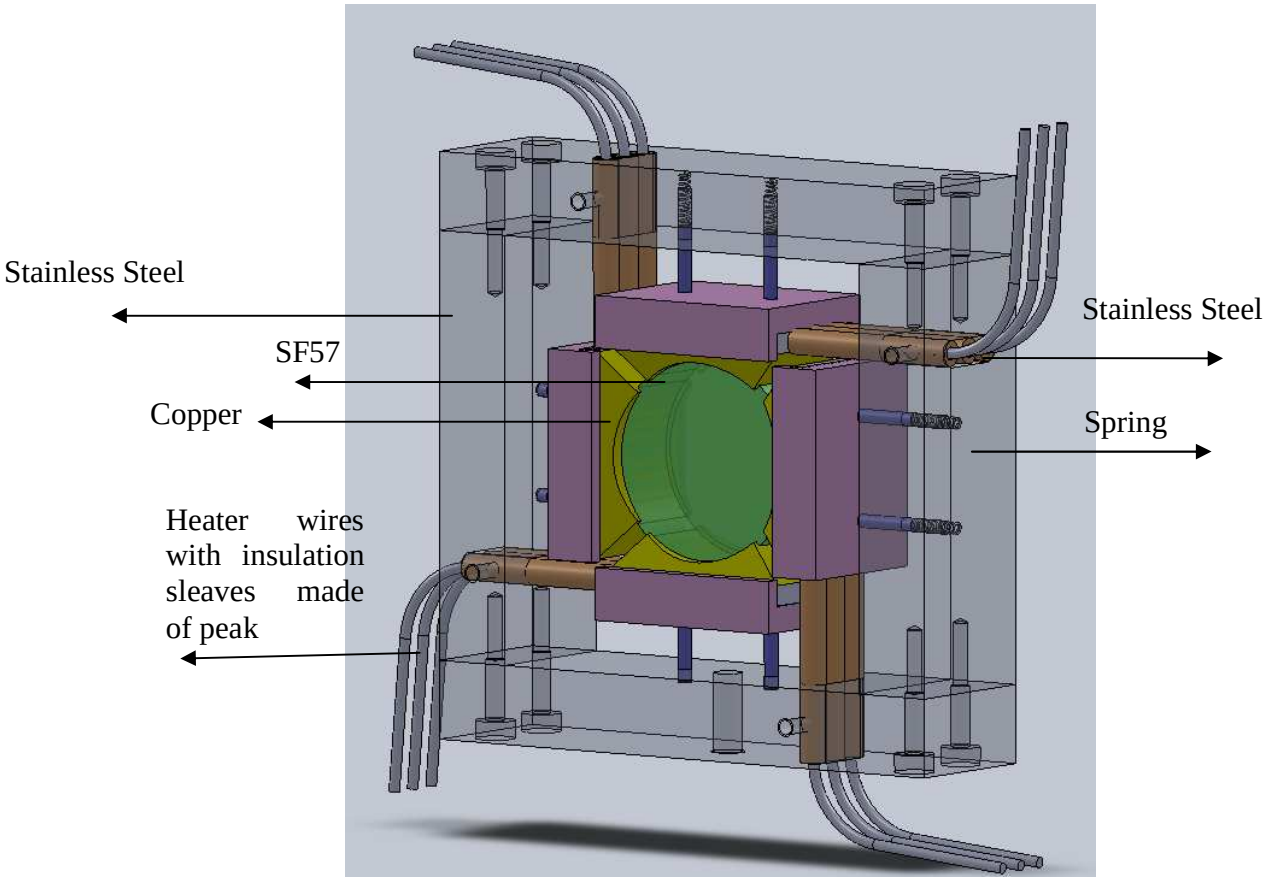

Fig. 3: Advanced LIGO AOE Assembly

3.2 Optical Element Specifications

SF57 will be used as the optical element due to its large dn/dT and thermal expansion coefficient. The low thermal conductivity of the material also helps in inducing more thermal lensing with given amount of heat. The comparison of SF57 with other candidate materials is given in Ref. 2. The material properties of SF57 are produced below.

Data Sheet

SCHOTT

SF57
847238.551

n_d = 1.84666	ν_d = 23.83	$n_F - n_C$ = 0.035536
n_e = 1.85504	ν_e = 23.64	$n_{F'} - n_{C'}$ = 0.036166

Refractive Indices

	λ [nm]	
$n_{2325.4}$	2325.4	1.79026
$n_{1970.1}$	1970.1	1.79539
$n_{1529.6}$	1529.6	1.80187
$n_{1060.0}$	1060.0	1.81185
n_t	1014.0	1.81335
n_s	852.1	1.82038
n_r	706.5	1.83102
n_C	656.3	1.83650
$n_{C'}$	643.8	1.83808
$n_{632.8}$	632.8	1.83957
n_D	589.3	1.84636
n_d	587.6	1.84666
n_e	546.1	1.85504
n_F	486.1	1.87204
$n_{F'}$	480.0	1.87425
n_g	435.8	1.89393
n_h	404.7	1.91366
n_i	365.0	
$n_{334.1}$	334.1	
$n_{312.6}$	312.6	
$n_{296.7}$	296.7	
$n_{280.4}$	280.4	
$n_{248.3}$	248.3	

Internal Transmittance τ_i

λ [nm]	τ_i (10mm)	τ_i (25mm)
2500	0.891	0.750
2325	0.910	0.790
1970	0.971	0.930
1530	0.996	0.991
1060	0.999	0.997
700	0.998	0.996
660	0.998	0.994
620	0.998	0.994
580	0.998	0.994
546	0.998	0.994
500	0.994	0.986
460	0.987	0.968
436	0.971	0.930
420	0.941	0.860
405	0.882	0.730
400	0.847	0.660
390	0.727	0.450
380	0.523	0.198
370	0.160	0.010
365	0.040	
350		
334		
320		
310		
300		
290		
280		
270		
260		
250		

Relative Partial Dispersion

$P_{s,t}$	0.1976
$P_{C,s}$	0.4539
$P_{d,C}$	0.2859
$P_{e,d}$	0.2356
$P_{g,F}$	0.6160
$P_{i,h}$	
$P'_{s,t}$	0.1942
$P'_{C',s}$	0.4895
$P'_{d,C'}$	0.2373
$P'_{e,d}$	0.2315
$P'_{g,F'}$	0.5443
$P'_{i,h}$	

Deviation of Relative Partial Dispersions ΔP from the "Normal Line"

$\Delta P_{C,t}$	-0.0065
$\Delta P_{C,s}$	-0.0046
$\Delta P_{F,e}$	0.0026
$\Delta P_{g,F}$	0.0123
$\Delta P_{i,g}$	

Constants of Dispersion Formula

B_1	1.81651371
B_2	0.428893641
B_3	1.07186278
C_1	0.0143704198
C_2	0.0592801172
C_3	121.419942

Constants of Dispersion dn/dT

D_0	$7.26 \cdot 10^{-6}$
D_1	$1.88 \cdot 10^{-8}$
D_2	$-5.14 \cdot 10^{-11}$
E_0	$1.96 \cdot 10^{-6}$
E_1	$1.79 \cdot 10^{-9}$
λ_{TK} [µm]	0.276

Color Code

λ_{80}/λ_5	40/37*
(*= λ_{70}/λ_5)	

Remarks

lead containing glass type. suitable for precision molding

Other Properties

$\alpha_{-30/+70°C}$ [10^{-6}/K]	8.3
$\alpha_{+20/+300°C}$ [10^{-6}/K]	9.2
T_g [°C]	414
$T_{10}^{13.0}$ [°C]	391
$T_{10}^{7.6}$ [°C]	519
c_p [J/(g·K)]	0.360
λ [W/(m·K)]	0.620
ρ [g/cm³]	5.51
E [10^3 N/mm²]	54
μ	0.248
K [10^{-6} mm²/N]	0.02
$HK_{0.1/20}$	350
HG	1
B	0
CR	2
FR	5
SR	52.3
AR	2.3
PR	4.3

Temperature Coefficients of Refractive Index

	$\Delta n_{rel}/\Delta T$[10^{-6}/K]			$\Delta n_{abs}/\Delta T$[10^{-6}/K]		
[°C]	1060.0	e	g	1060.0	e	g
-40/ -20	6.6	11.1	16.7	4.2	8.6	14.1
+20/ +40	7.6	12.5	18.9	6.0	10.9	17.2
+60/ +80	8.0	13.4	20.1	6.8	12.1	18.8

As of /06/30/2003, Subject to change

SF57 is a low cost material with low absorption. The measured absorption of SF57 is found to be 125 ± 25 ppm/cm. As explained in Ref. 2, the FOM defined as:

$$\text{FOM} = \left[\frac{dn}{dT} + \alpha_T(1+\upsilon)\times(n-1)\right]\left[\frac{1}{\kappa}\right] = 25.1\mu m/W$$

or

$$Sag = P_{abs}\times\frac{FOM}{4\pi}$$

For 125 W and 125 ppm/cm absorption and 1 cm long SF57, the absorbed power is 16 mW. This corresponds to a sag of 32 nm or approximately λ/34 for 1064 nm. For a 2 mm beam size, this sag corresponds to 30 m focal length, or about 1/3 or the dynamic range available from SF57. However, it should be noted this thermal lensing will taken into account while designing the DKDP thickness in FI. A slightly larger thickness of DKDP can be used to off-set the self thermal lensing in the SF57. The thermal lensing is low enough to the extent that it does not introduce higher order losses. As a comparison, the expected thermal lensing from TGG is about 15 m per crystal.

3.2.1 Dimensions

The exact dimensions of the optics are:

Thickness: 1 cm

Diameter: 2.54 cm

3.2.2 Polishing and Coating

The SF57 comes as a blank from Schott glass. Our last batch was AR coated from:

PRECISION PHOTONICS CORPORATION

3180 Sterling Circle

Boulder, CO 80301

The measured upper-bound of AR reflectivity is 500 ppm per surface. The company claims this value to be under 300 ppm. The AR coating changes with temperature and drops to about 1000 ppm per surface at 200^0C. Because of the slow response, this is not expected to pose a problem. However, we are looking for better thermally stable coatings for Advanced LIGO.

The polishing surface quality will be similar to other transmissive elements in IO such as TGG and DKDP. The surface flatness should be better than λ/10 (for 633 nm). The scratch/dig specification should be better than 10-5.

3.2.3 Response Time

The measured and modeled response time of the AOE in response to the application of a step function heating is found to be around 500 seconds.

3.2.4 Location

We are proposing to reserve space for two AOE in Advanced LIGO. However, initially we will install only one AOE. The reason for proposing two AOEs is to offer flexibility, i.e., to provide two

dynamic lenses (‘control knobs’) in the IO for dynamic mode matching into the RC in future. If there is any residual thermal lensing in RC that TCS can not compensate, having two knobs enable us to mode match to various power levels for low power operation. This is an ongoing effort and will be coordinated along with our TCS collaboration. Another advantage of two elements is that the IO section can be tuned to low power operation where the best mode matching is achieved at some low power level say 25 W compatible with the Advanced LIGO low power operation mode.

However, for the initial installation, we use one AOE to test the feasibility of AOE under real AdvLIGO conditions. The location selected is after SM_1. The details are provided in Ref. 1.

3.2.5 Range

The range of AOE is tested in lab and the results are summarized in Ref. 1 and 2 and are shown in Fig. 4 for reference.

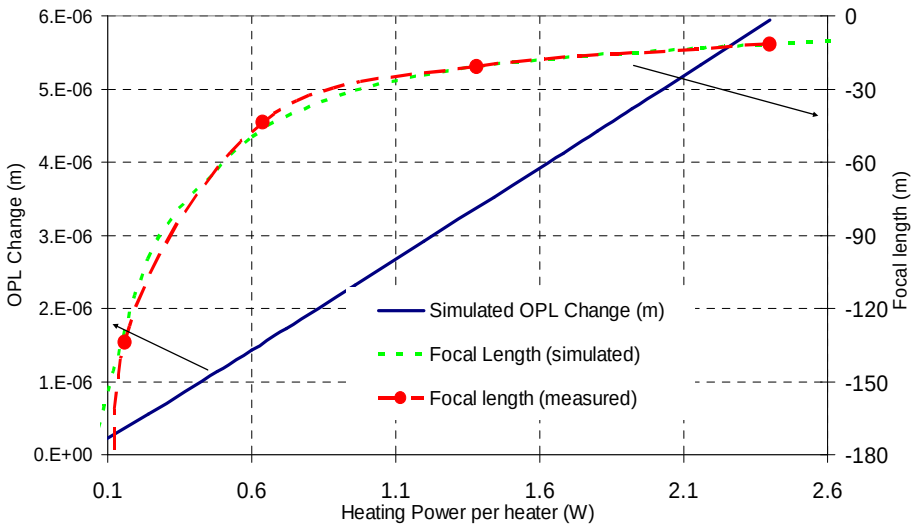

Fig. 4. Estimated lensing based upon Fig. 4 data calculated by means of ABCD matrices. The solid blue line shows the cumulative *OPL* change between the center and the edge of the lens while dotted green line represents the simulated focal length (m) as a function of heating power. The measured data shown in dashed red curve shows very good agreement with the simulations.

A thermal lens of 10 m can be obtained by putting 2.4 W per heater. This provides sufficient control of the ROC errors in the IO section.

We have tested SF57 up to 200^0C and have not seen any visible damage to the material. SF57 being a glass, can tolerate relatively higher temperature than crystals. However, SF57 has a large thermal expansion coefficient; therefore, the mounting of SF57 is critical. In the design of the SF57 mount, we have provided a spring-loaded arrangement to release the stress. Additionally, the temperature monitoring system will sense the temperature of SF57 and in case of malfunction. i.e., temperature higher than 200^0C, the heat input to the system will be cut-off. We have also tested

SF57 at 80 W of laser power and we plan to conduct additional test at high power laser beam at 125 W (using a double pass geometry) to test the damage threshold of SF57 for CW light.

3.2.6 Vacuum Compatibility

SF57 is a optical glass so we expect that this will be vacuum compatible. It has been tested at UF at moderate vacuum (10^{-6} torr). More elaborate tests will be conducted at HPLF in the coming months.

3.2.7 Beam Centering and Alignment Considerations

The rms centering requirement at the ITM for the relative movement of the beam is about 1 mm. Given the ABCD matrices between IO and ITM, this becomes 50 μm beam drift requirement at SM_1 or a 3 μrad angular misalignment at the AOE. We model the AOE as a thick lens and derive equivalent beam centering requirements.

The results are summarized in Fig. 5. The blue line is the resultant beam drift from misalignment from SF57 when no lens is present and red lines corresponds to -10 m len which is the maximum range of SF57. It is apparent that the more stringent restriction is provided by the 1 mm beam displacement requirement at the ITM. With no lens, this is 50 μm while with -10 m lens, the beam centering requirement becomes 20 μm.

The beam decentering can occur due to two reasons.

1. Due to relative motion of HAM table
2. Due to physical misaligned heaters and the beam path

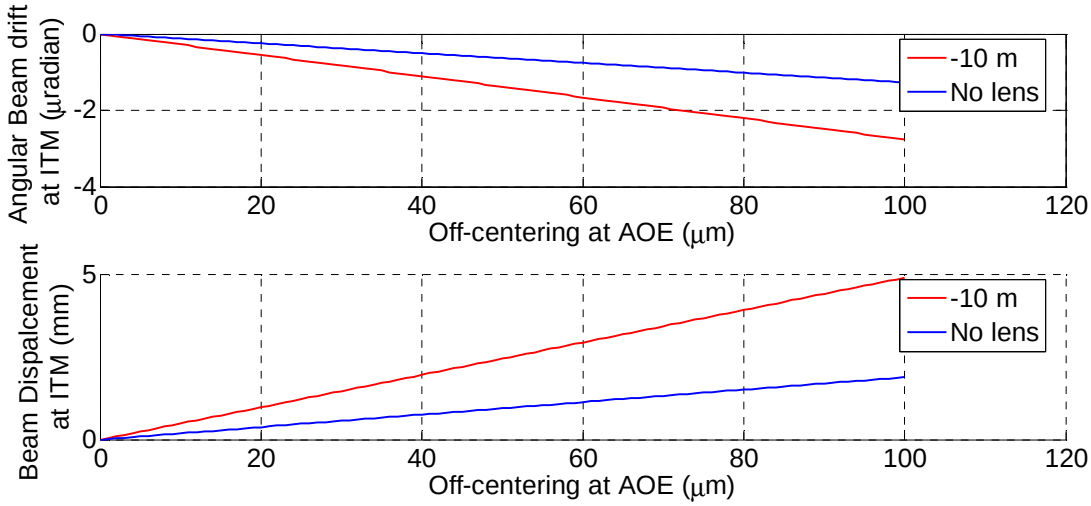

Fig. 5: Calculation of beam jitter from AOE at ITM in terms of beam displacement and angular misalignment. The first plot represents the angular misalignment while the second plot shows beam displacement.

HAM motion is well under 20 μmeter rms. The requirement for centering the beam on AOE has been tested in the lab. The beam can be aligned to the AOE by two methods. Initially the beam can be put physically in the center of SF57. Once it has been installed in vacuum, the center of the

beam can itself be changed by changing the relative heating. This is shown in Ref. 2. Since we may need to tilt SF57 to avoid AR reflections scattering back, we tested SF57 under various tilt angles, as shown in Fig. 6.

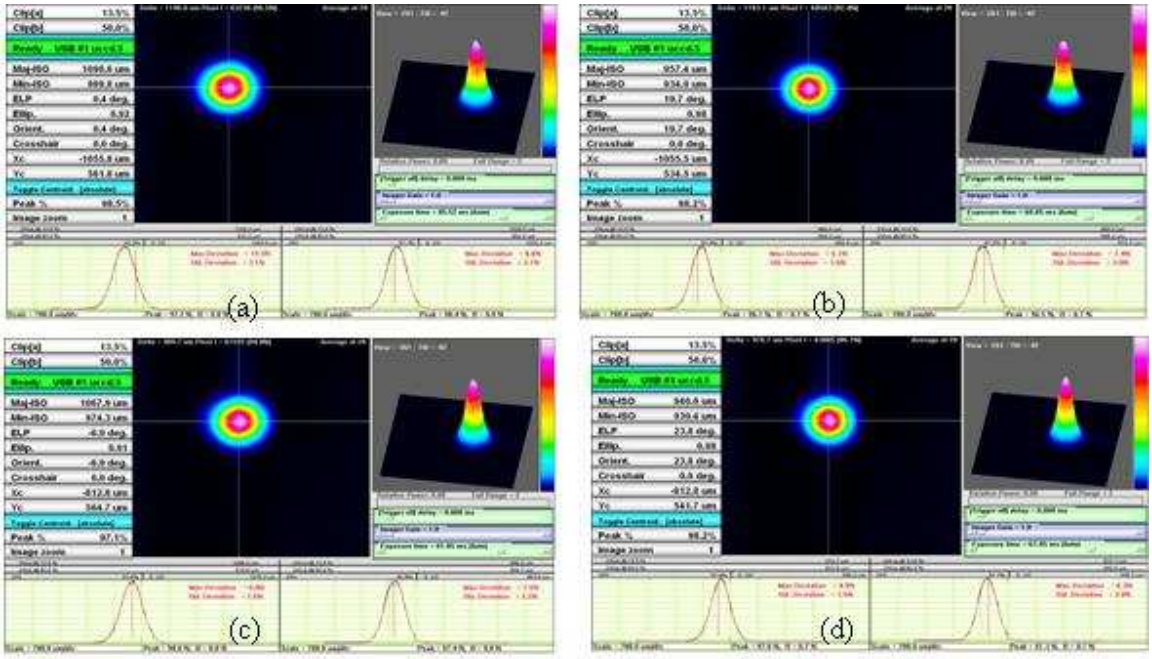

Fig. 6: Images of beam passing through SF57 at: a) normal incidence and full heating power, b) normal incidence and no heating power, c) 20 degree AOI at full power, and d) 20 degree AOI at no power. The centroid location shows beam displacement.

Although it is hard to see in Fig. 6, analysis shows that the centroid of the beam with full heating stays within 1 μm of the original position from no heating to full heating. Using standard ABCD matrices, including one for a tilted thick lens, we can estimate the corresponding off-centering of the beam at the input. It is estimated that the beam was centered within 8 μm of the lens center. Note that we centered the beam first by hand on SF57 and then measuring the beam deviation at a fixed point and changing the voltage levels to the heaters to shift the center of the lens. Once the alignment procedure was complete, the balance of the power and manual alignment was not shifted during heating/no heating. In fact SF57 was kept on a rotational stage and alignment was not changed during various tilt angles. The 8 μm number is an order of 2.5 lower than the requirement. Therefore SF57 beam centering will meet Advanced LIGO requirements.

3.2.8 Alignment procedure and calibration

For the initial alignment, we put the AOE at the designated location and ensures that the beam was passing through the center of the optic. A more precise alignment can be done once the AOE is under use in vacuum. A pair of QPDs (QPD_IOA1 and QPD_IOA2 on IOT) is provided to measure the beam coming from AOE. A GigE camera also looks at the beam image on the SF57 (BSS2 on IOT) to provide centroid information. The details can be found in Ref. 5 and 6 for both straight and folded interferometers. A procedure adopted for precise alignment is described in Ref. 4.

4 Description of Ring Heaters

Another essential component of the AOE is the ring heater. We have tested various units.

1. Minco based Kapton supported heaters
2. Watlow slab heaters
3. Nichrome strip heaters
4. vacuum deposition of Nichrome
5. Advanced Ceramic heater (ULTRAMIC^{TM} 600) from Watlow.

Out of these we found the Ultramic heaters the most suitable.

4.1 Ultramic^{TM} 600 heaters Specification

These heaters are constructed of Aluminum Nitride (AlN). These heaters are specially designed for applications requiring a clean and non-contaminating heat source and can be used for heating up to 600^0C with ramp rates as high as 150^0C per second. They come with a built-in thermocouple that can be used for temperature measurements. The model we have chosen is

Model: CER-1-01-00098

Size: 25 mm x 15 mm x 2.5 mm

Watts: 180

Max. Voltage: 120 V

Resistance: 85 ohm

4.1.1 Operating Conditions

We expect that the maximum power to the heater will 4 W; this gives 200^0C temperature. Thus the full load operating conditions will be:

Voltage: 25 V

Current: 220 mA

These requirements are very easy to meet. A fairly ordinary power supply will suffice. It is noted that a lensing error of -100 m ROC only produces about 0.5% mode mismatch which is tolerable. A -100 m ROC can be obtained by applying approximately 2.5 V. Therefore the needed stability of the voltage source is about 10%. The time constant of AOE is around 500 s. Hence no frequency stabilization is necessary for the voltage source.

4.1.2 Temperature readout

The internal temperature readout in the Watlow Ultramic heater is a k-type thermocouple, integrated into the heater. We had some discussions with CDS where concerns were raised about the suitability of a thermocouple for temperature measurements in vacuum. Noise can be an issue

with the thermocouples. However, the temperature measurements are a safety mechanism. The accuracy requirements are not of great concern. We would like to put a safety stop that if the temperature gets higher than 200^0C, the heater power is shut down. At these higher levels of temperatures, the noise contribution becomes even smaller as the signal strength goes up. For now the baseline is to use the built-in thermocouple but we are looking into alternate solution where we can put a CDS-preferred RTD in the system for temperature measurements.

The temperature profile of the heater when heated to 200^0C is shown in Fig. 7. Fig. 7 shows that the temperature gradient dies out at about 6 cm from the heater.

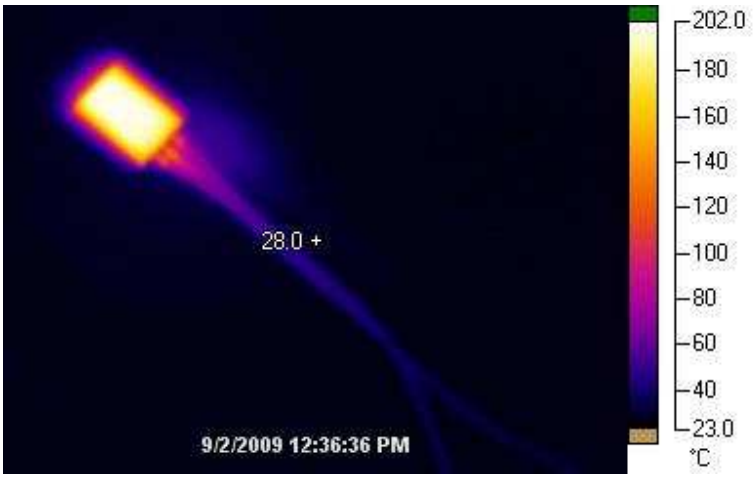

Fig. 7: Thermal image of the heater when heated to 2000C. The image also shows the wire temperature.

5 QPD for Alignment

The Quad photodetector is placed on the IOT1 table and will be used to measure the beam centering on AOE_1. The detectors are designated as QPD_IOA1 and QPD_IOA2. The location can be found in the IOT layout drawings. [See Refs. 5 and 6].

6 Test Plan

The inspection, cleaning, and baking will be done following IO optics inspection guidelines for other in-vacuum transmissive optics. The calibration procedure outlined in Sec. 3.2.8 and described in Ref. 4 measures the alignment of the AOE. Once the calibration procedure is done, the AOE will be tested for dynamic operation. There are two aspects of AOE thermal lensing tests.

1. Self thermal lensing
2. Heater-induced thermal lensing

6.1 Self thermal lensing

1. The SF57 will be tested at HPLF using high power laser beam in double pass geometry to evaluate the performance at high power levels.
2. Self lensing will be measured and calibrated.

3. SF57 in combination with FI (with DKDP) will be tested for high power operation. This ensures optimal performance for thermal lensing, thermal depolarization, and mounting issues.
4. In-vacuum testing will be performed as outlined in Ref. 7 in combination with general IO reliability and mode matching testing.

6.2 Heater induced thermal lensing

1. Prior to installation, AOE will be tested in vacuum for full dynamic range testing. Beam scan measurements, response time analysis, beam quality analysis will be performed for various power levels.
2. Thermal images of the SF57 element under various heating loads will be evaluated. The thermal imaging technique will be very useful in analyzing any asymmetries in the heating profile.
3. Once installed in vacuum and tested for alignment, the AOE will be tested *in-situ*. This is done by using a lower power beam with PRM misaligned. A low power level (say 1 W at IMC output) will ensure that the self thermal lensing is low.
4. The beam, after passing through AOE, will be incident at SM_2.
5. The transmission through SM_2 is relayed to IOT where we have designated mode matching sensor BSS2.
6. The beam size at BSS2 will be measured as a function of heating power and a chart/table will be prepared to calibrate the thermal performance in terms of electrical heating.
7. The calibration procedure (mentioned in Sec. 3.2.8 and in Ref. 4) also notes the bias to be applied for proper centering of the heating profile.
8. Additionally, a beam scan on IOT will be performed to confirm the beam size change information. Note that a designated space has been reserved on the IOT for Bulls eye/beam scan measurements.
9. The data obtained from the thermal lensing measuring will be compared with the expected results to identify any potential problems.
10. The temperature measurement system in place as a safety measure will be tested and the shut-off procedure will be verified to affirm that the heating is stopped if the temperature rises above 200^0C.

7 CDS Interface

For operation of the AOE, we require the following

1. 4 channel per AOE for heater input and monitoring (provision for two AOEs per IFO)

(25 V, 500 mA maximum)

2. 4 channel for temperature measurements per AOE
    A. baseline: K type built-in thermo couple
    B. External RTD mounted with the heaters
3. QPD Readout from IOT

The location and specifications of the elements mentioned above are defined in Ref. 1.

8 Summary

We have presented the engineering specification of the proposed AOE in IO of Advanced LIGO. Specific issues such as type of heaters, optical element, heater control, and temperature readout are discussed. The interface with CDS is defined.